
Learning vector autoregressive models with focalised Granger-causality graphs

Magda Gregorova

HES-SO & University of Geneva, Switzerland
magda.gregorova@unige.ch

Alexandros Kalousis

HES-SO & University of Geneva, Switzerland
alexandros.kalousis@unige.ch

Stéphane Marchand-Maillet

University of Geneva, Switzerland
stephane.marchand-maillet@unige.ch

Jun Wang

Expedia, Geneva, Switzerland
jwang1@expedia.com

Abstract

While the importance of Granger-causal (G-causal) relationships for learning vector autoregressive models (VARs) is widely acknowledged, the state-of-the-art VAR methods do not address the problem of discovering the underlying G-causality structure in a principled manner. VAR models can be restricted if such restrictions are supported by a strong domain theory (e.g. economics), but without such strong domain-driven constraints the existing VAR methods typically learn fully connected models where each series is G-caused by all the others. We develop new VAR methods that address the problem of discovering structure in the G-causal relationships explicitly. Our methods learn sparse G-causality graphs with small sets of *focal* series that govern the dynamical relationships within the time-series system. While maintaining competitive forecasting accuracy, the sparsity in the G-causality graphs that our methods achieve is far from reach of any of the state-of-the-art VAR methods.

1 Introduction

In this paper we develop methods for learning vector autoregressive models (VARs) for forecasting multiple time series based solely on their past observations together with discovering the Granger-causality (G-causality) graphs describing the relationships amongst the series. The VARs are well established models in the time series literature (e.g. [1]), yet the problem of discovering the underlying G-causality relationships is not satisfactorily addressed by the existing VAR learning methods.

The G-causality refers to a specific type of *predictive* relationship amongst the series. In brief, time series Z is said to G-cause time series Y if Y can be better forecast using the past of Z than without it. The graph of such relationships is naturally captured within the parameters matrix of a VAR model. When learning VARs, zero equality constraints can be imposed on the parameters matrix to restrict the model learning to G-causal graphs corresponding to the specific domain theory (e.g. macroeconomic theory). However, the problem of discovering the G-causal graphs in the absence of such domain-driven assumptions is not addressed by the state-of-the-art methods in a principled manner and most often the learned VARs have fully connected G-causal graphs.

We propose here and develop methods to learn VARs with *focalised* G-causal graphs, i.e. *sparse* graphs with a small number of *focal* series - vertices with out-edges. The sparsity motivation follows from the need to control the complexity of the models as VARs typically suffer from the high-dimensionality-low-sample problem. Sparse models and graphs have clear interpretational advantages, and forecasting based on sparse models is also computationally cheaper. The motivation for the focalised structure comes from the fact that VARs are typically used for systems of closely

related series (e.g. generated from a single complex process) and as such are likely to be subject to the same (or similar) forces driving their dynamics - the focal series. This sharing of focal series across models (or across groups of models) naturally leads to the need to learn the models jointly in a multi-task manner. By intertwining the sparse learning across the models towards the common focal series we also stabilise the variable selection [2].

After describing the VARs and G-causality more formally in sections 1.1 and 1.2, we introduce in section 2 two new methods for learning VARs with focalised G-causal graphs. To begin with, in 2.1 we assume that the focal series are common to all the predictive tasks. Since this may not be a realistic assumption in many real life applications, we develop in section 2.2 an additional soft-clustering variant which discovers soft model clusters based on sets of common focal series. We test the validity of our structural assumptions for the VARs and the learning ability of our methods in a set of experiments on real data in section 4 where we show that we achieve forecasting performance at least as good as other state-of-the-art VAR methods while at the same time we discover much sparser G-causal graphs with typically very small numbers of focal series.

Our work builds on the ideas of clustered multi-task and sparse structured learning [3, 2, 4] adapting them for the specific problem of VAR and G-causality learning. While there exist many other valid time series modelling approaches, we limit our attention here to VARs, which belong to the standard multiple time series modelling tool-set, with the aim to improve upon the existing methods for their learning. More detailed review of the related work is given in section 3.

1.1 Vector autoregressive model

For a set of K time series observed at T synchronous equidistant time points, we write the VAR in the form of a multi-output regression problem as

$$\mathbf{Y} = \mathbf{X}\mathbf{W} + \mathbf{E}, \quad (1)$$

where \mathbf{Y} is the $T \times K$ output matrix for T instances and K time series as individual forecasting tasks, \mathbf{X} is the $T \times Kp$ input matrix so that each row t of the matrix is a Kp long vector with p lagged values of the K time series as inputs $\mathbf{x}_{t,\cdot} = (y_{t-1,1}, y_{t-2,1}, \dots, y_{t-p,1}, y_{t-1,2}, \dots, y_{t-p,K})'^1$, and \mathbf{W} is the corresponding $Kp \times K$ parameters matrix where each column is a model for a single time series forecasting task. We follow the standard time series assumptions: the $T \times K$ error matrix \mathbf{E} is a random Gaussian noise matrix with i.i.d. rows $\mathbf{e}_{t,\cdot} \sim N(\mathbf{0}, \Sigma)$; the time series are second order stationary and centred (so that we can omit the intercept).

In principle, we can estimate the model parameters by minimising the standard squared error loss

$$L(\mathbf{W}) := \sum_{t=1}^T \sum_{k=1}^K (y_{t,k} - \langle \mathbf{w}_{\cdot,k}, \mathbf{x}_{t,\cdot} \rangle)^2 \quad (2)$$

which corresponds to maximising the likelihood with i.i.d. Gaussian errors. However, since the dimensionality Kp of the regression problem quickly grows with the number of series K (by a multiple of p), usually already relatively small VARs are highly over-parametrised ($Kp \gg T$) and some form of regularisation needs to be used to condition the model learning.

1.2 Granger-causality graphs

In [5] the author defines causality based on the predictability of the series: we say that Z causes Y if we can forecast Y better using the history of X than without it. Such a predictability based view of causality has become known as the Granger-causality (G-causality). It can be extended to sets of series so that a set of series $\{Z_1, \dots, Z_l\}$ is said to G-cause series Y if Y can be better predicted using the past values of the set.

The G-causal relationships can be described by a directed graph $\mathcal{G} = \{\mathcal{V}, \mathcal{E}\}$ in which the set of vertices represents the time series in the system, and a directed edge $e_{l,k}$ from v_l to v_k means that time series l G-causes time series k . The graphs we propose to learn by our methods developed in section 2 are sparse and focalised - they have a small number of vertices with out-edges.

¹By convention, all vectors in this paper are column vectors.

In VARs the G-causal relationships are captured within the \mathbf{W} parameters matrix of model (1). When any of the parameters of the k -th task (k -th column of the \mathbf{W}) referring to the p past values of the l -th input series is non-zero, we say that the l -th series G-causes series k , and we denote this in the G-causality graph by a directed edge $e_{l,k}$ from v_l to v_k . In this way, it is possible to read the G-causality graph directly from the learned \mathbf{W} matrix of a VAR model (see figure 1).

2 Multi-task learning in VAR

In multi-task learning (MTL) we benefit from sharing information amongst the tasks as opposed to learning the tasks in isolation. Building on the MTL ideas we develop two methods for learning VARs with sparse focalised G-causal graphs. To strike the best balance between the two learning extremes (independent models vs single common model) we allow each of the task models to have a *common* and a *task-specific* component. The common learning part captures the similarity of the models with respect to the G-causal relationships, more precisely the G-causing series - the focal series in the G-causal graph. The task-specific part lets the models to diverge in their parameter values in \mathbf{W} (weights for the focal series) and lets each of the series depend on its own history (a common assumption in time series forecasting).

2.1 Focalised-VAR

In the first method we assume that *all tasks have the same common part* of the model, i.e. that all the task models have the same focal series in the sparse G-causal graph (assumption 1). However, the models can still differ due to the task-specific components: weights for focal series in \mathbf{W} and dependency on own past. We call this method the Focalised-VAR (F-VAR).

We translate the above assumptions for F-VAR into the structural properties of the parameters matrix \mathbf{W} of model (1) (see figure 1): it shall be a sparse matrix with common non-zero *blocks* of rows across all the columns (common focal series for all the models) and with full *block*-diagonal elements (task-specific own past). The blocks are naturally defined from the structure of the VAR model: the input matrix \mathbf{X} contains the shifted (lagged) values of the time series and a block in \mathbf{X} corresponds to a single input time series with all its lags up to p steps back; this carries directly over to \mathbf{W} so that a block in \mathbf{W} has the parameters of the corresponding block in \mathbf{X} .

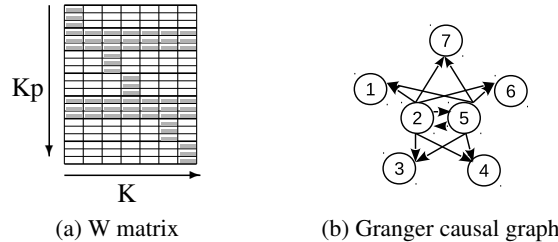


Figure 1: Schematic structure of a focalised parameters matrix \mathbf{W} and the corresponding G-causality graph for a system of $K = 7$ series. In (a), the number of lags is $p = 3$, the gray cells are the non-zero elements, series 2 and 5 are the focal series. In (b), the focal series are the vertices in the center of the graph (self-loops corresponding to the block-diagonal elements in \mathbf{W} are omitted for clarity of display).

To formulate our learning problem, we begin with partitioning the input vectors $\mathbf{x}_{t,\cdot}$ in eq. (2) into the block sub-vectors $\mathbf{x}_{t,\cdot} = (\tilde{\mathbf{x}}'_{t,1}, \tilde{\mathbf{x}}'_{t,2}, \dots, \tilde{\mathbf{x}}'_{t,K})'$ so that the k th block contains all lagged values of series k , and we rewrite the inner product in eq. (2) using these sub-vectors $\langle \mathbf{w}_{\cdot,k}, \mathbf{x}_{t,\cdot} \rangle = \sum_{b=1}^K \langle \tilde{\mathbf{w}}_{b,k}, \tilde{\mathbf{x}}_{t,b} \rangle$. We then decompose each of the sub-vectors $\tilde{\mathbf{w}}_{b,k} = \gamma_{b,k} \tilde{\mathbf{v}}_{b,k}$ into the product of a scalar $\gamma_{b,k}$ and a same dimension vector $\tilde{\mathbf{v}}_{b,k}$ and rewrite the loss function in terms of these

$$L(\Gamma, \mathbf{V}) := \sum_{t=1}^T \sum_{k=1}^K (y_{t,k} - \sum_{b=1}^K \gamma_{b,k} \langle \tilde{\mathbf{v}}_{b,k}, \tilde{\mathbf{x}}_{t,b} \rangle)^2 \quad (3)$$

In this way, we have introduced the necessary block-structure into the loss function, and we have provided ourselves with the means to control the sparsity in \mathbf{W} at the desired block-level through the $K \times K$ matrix $\mathbf{\Gamma}$.

As explained above, the structural sparsity assumptions for our models are composed of two parts: the common part assumes that all models have the same focal series (blocks of rows in \mathbf{W}), the task-specific part enables the models to always depend on their own past (block-diagonal in \mathbf{W}). To bring this dichotomy into our method, we decompose the structural matrix $\mathbf{\Gamma}$ into two $K \times K$ matrices: a sparse matrix \mathbf{A} with the same sparsity pattern (that we need to learn) in all its columns (models) $\alpha_{.,k} = \bar{\alpha}, \forall k$ capturing the common part of the structural assumptions about the same focal series participating in all the models; and a diagonal matrix $\mathbf{B} = \tau \mathbf{I}$ capturing the task-specific part about the models always depending on their own past. We tie the matrices together by $\mathbf{\Gamma} = \mathbf{A} - \text{diag}(\mathbf{A}) + \mathbf{B}$, where the middle term frees the diagonal elements from the common learning of \mathbf{A} and thus leaves them to be specified by the \mathbf{B} . We choose to set $\tau = 1$ in all the following².

We now state our optimisation problem as a constrained minimisation of the loss function (3)

$$\underset{\mathbf{\Gamma}, \mathbf{V}}{\text{argmin}} L(\mathbf{\Gamma}, \mathbf{V}) \quad \text{s.t.} \quad \mathbf{1}'_K \bar{\alpha} = 1; \bar{\alpha} \geq \mathbf{0}; \|\mathbf{V}\|_F^2 \leq \epsilon \quad (4)$$

where $\|\cdot\|_F$ is the Frobenious norm, $\mathbf{1}_K$ is a K -long vector of ones, $\mathbf{\Gamma} = \mathbf{A} - \text{diag}(\mathbf{A}) + \mathbf{I}$, and $\alpha_{.,k} = \bar{\alpha}$ for all k .

In (4) we impose a standard ridge penalty [6] on the \mathbf{V} matrix, but it is the simplex constraint on the common $\bar{\alpha}$ vector which plays the most important role here in promoting sparsity in the final \mathbf{W} matrix at the pre-specified block-level. We use the unit simplex to achieve identifiability.

We solve the non-convex optimisation problem (4) to find a local minimum by alternating descent for \mathbf{V} and $\bar{\alpha}$ as outlined in algorithm 1. We initialize \mathbf{V} as the ridge estimate and $\bar{\alpha}$ evenly so that $\alpha_b = 1/K$ for all b .

Algorithm 1 Focalised-VAR **Input:** $\mathbf{Y}, \mathbf{X}, \lambda$; initialize \mathbf{V} and $\bar{\alpha}$.

repeat

 Step 1: Solve for \mathbf{V}

 put $\alpha_{.,k} = \bar{\alpha}$ for all columns of \mathbf{A}

 get $\mathbf{\Gamma} = \mathbf{A} - \text{diag}(\mathbf{A}) + \mathbf{I}$

 re-weight input blocks $\mathbf{z}_{t,b,k} = \gamma_{b,k} \tilde{\mathbf{x}}_{t,b}$.

 solve for each k $\|\mathbf{y}_{.,k} - \mathbf{Z}_k \mathbf{v}_{.,k}\|_2^2 + \lambda \|\mathbf{v}_{.,k}\|_2^2$

 Step 2: Solve for $\bar{\alpha}$

 get block products $h_{t,b,k} = \langle \tilde{\mathbf{v}}_{b,k}, \tilde{\mathbf{x}}_{t,b} \rangle$

 get residuals $r_{t,k} = y_{t,k} - h_{t,k,k}$ using own history

 concatenate $h_{t,b,k}$ into $T \times K$ matrix \mathbf{H}_k and replace k th column in \mathbf{H}_k by zeros

 concatenate \mathbf{H}_k matrices into $KT \times K$ matrix \mathbf{H}

 solve $\text{vec}(\mathbf{R}) = \mathbf{H} \bar{\alpha}$, s.t. simplex constr. on $\bar{\alpha}$

until convergence

2.2 SoftFocalised-VAR

Assumption 1 used in the previous section is very restrictive and hardly realistic in many real life applications. Therefore we relax it here for our second method, the SoftFocalised-VAR (SF-VAR), and we assume instead that the task models can be clustered by the focal series they have in common³

If the model clustering were known a priori (e.g. from domain knowledge), it could be incorporated into problem (4) fairly easily (we call this approach *clustered* F-VAR) by associating each of the C clusters with a sparsity vector $\bar{\alpha}^c$ and setting $\alpha_{.,k} = \bar{\alpha}^c$ for all tasks k belonging to cluster c . We

²Note that $\tilde{\mathbf{w}}_{b,k} = (\tau \gamma_{b,k}) (\tilde{\mathbf{v}}_{b,k} / \tau)$, and $\gamma_{b,k} = \beta_{k,k}$. Alternatively, we could have treated τ as a hyper-parameter controlling for the relative weight of own past compared to the past of the neighbouring series and learn it.

³We leave the task-specific assumptions unchanged.

then learn all $\bar{\alpha}^c$ by slight modification of step 2 in algorithm 1: instead of matrices \mathbf{H} and \mathbf{R} , we construct C matrices \mathbf{H}^c as concatenations of $\mathbf{H}_k, k \in c$ and \mathbf{R}^c as concatenations of $\mathbf{r}_{\cdot,k}, k \in c$, and we solve C problems $\text{vec}(\mathbf{R}^c) = \mathbf{H}^c \bar{\alpha}^c$ with simplex constraints on $\bar{\alpha}^c$. In reality, the task clustering is usually not available a priori and needs to be discovered together with learning the models - this is what our SF-VAR described here below achieves.

For the SF-VAR method we relax the strict equality link between the columns of \mathbf{A} used in section 2.1 for F-VAR and instead assume that the columns live in a lower dimensional subspace spanned by r sparse K -long vectors $\mathbf{d}_{\cdot,j}, j = \{1, \dots, r\}$ forming a $K \times r$ dictionary matrix \mathbf{D} with $r \leq K^4$. The dictionary atoms can be seen as the sparse cluster prototypes on which the individual task models draw by sparse linear combinations with weights specified in $r \times K$ matrix \mathbf{G} so that $\mathbf{A} = \mathbf{D}\mathbf{G}$. To learn the task models we do not learn the columns of the matrix \mathbf{A} directly as in problem (4) but rather learn the dictionary and weights matrices \mathbf{D} and \mathbf{G} , both with simplex constraints so that the resulting \mathbf{A} is low rank with columns on the simplex.

Figure 2(a) illustrates the *soft-clustering* effect of the $\mathbf{D}\mathbf{G}$ decomposition in SF-VAR and contrasts it with the clustered F-VAR with known clusters in 2(b) for which \mathbf{G} is the $C \times K$ binary matrix with the a priori known task-cluster assignments.

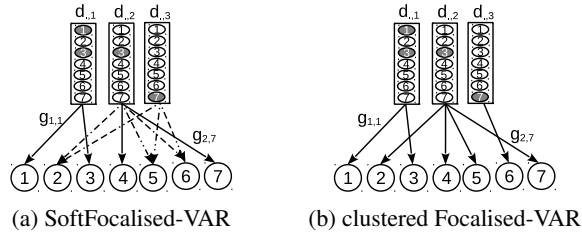


Figure 2: Schemas of the role of the \mathbf{D} and \mathbf{G} matrices in the (a) SoftFocalised-VAR and (b) clustered Focalised-VAR methods for an imaginary system with $K = 7$ time series and rank $r = 3$ matrix \mathbf{A} . The \mathbf{d} columns are the sparse cluster prototypes, the non-zero elements are shaded. The numbered circles in the bottom are the individual task models, the arrows are the elements of the weight matrix \mathbf{G} . Solid arrows have weight 1, dashed arrows have weights between 0 and 1.

We summarise the steps above into the new optimisation problem for the SF-VAR method

$$\underset{\mathbf{\Gamma}, \mathbf{V}}{\operatorname{argmin}} L(\mathbf{\Gamma}, \mathbf{V}) \quad \text{s.t. } \mathbf{1}_K' \mathbf{d}_{\cdot,j} = 1 \quad \forall j; \quad \mathbf{d}_{\cdot,j} \geq \mathbf{0} \quad \forall j; \quad \mathbf{1}_r' \mathbf{g}_{\cdot,k} = 1 \quad \forall k; \quad \mathbf{g}_{\cdot,k} \geq \mathbf{0} \quad \forall k; \quad \|\mathbf{V}\|_F^2 \leq \epsilon \quad (5)$$

where $\mathbf{A} = \mathbf{D}\mathbf{G}$, and $\mathbf{\Gamma} = \mathbf{A} - \text{diag}(\mathbf{A}) + \mathbf{I}$.

We find a local minimum of the non-convex problem (5) similarly as in algorithm 1 by alternating descent for \mathbf{V} (step 1 of the algorithm 1), and \mathbf{D} and \mathbf{G} in step 2. We initialise \mathbf{V} as the ridge estimate and the matrices \mathbf{D} and \mathbf{G} evenly so that $d_{ij} = 1/K$ and $g_{ij} = 1/r$ for all i, j . For a given \mathbf{D} , we solve for each task the simplex constrained least squares problem $\mathbf{r}_{\cdot,k} = \mathbf{H}_k \mathbf{D} \mathbf{g}_{\cdot,k}$, where $\mathbf{g}_{\cdot,k}$ is the k th column of \mathbf{G} . For a given \mathbf{G} , we solve the simplex constrained joint vectorised least squares problem $\text{vec}(\mathbf{R}) = \hat{\mathbf{G}} \odot \hat{\mathbf{H}} \text{vec}(\mathbf{D})$, where \odot is the Hadamard product, $\hat{\mathbf{G}} = \mathbf{G}' \otimes \mathbf{1}_T \mathbf{1}_K'$, $\hat{\mathbf{H}} = \mathbf{1}_r' \otimes \mathbf{H}$, and \otimes is the Kronecker product. We solve the simplex constrained least squares problems by projected gradient descent method with backtracking stepsize rule [7].

To understand better the effects of our methods on the VAR learning we can link our formulations to some other standard learning problems though bearing in mind that these have different aims and different assumptions than ours. We can rewrite the inner product in the loss function (3) as $\langle \tilde{\mathbf{v}}_{b,k}, \gamma_{b,k} \tilde{\mathbf{x}}_{t,b} \rangle$. In this "feature learning" formulation, the vectors $\gamma_{\cdot,k}$ act as weights for the original inputs and, hence, generate new (task-specific) features $\mathbf{z}_{t,b,k} = \gamma_{b,k} \tilde{\mathbf{x}}_{t,b}$ (see also algorithm 1). Alternatively, we can express the ridge penalty on \mathbf{V} used in eq. (5) as $\|\mathbf{V}\|_F^2 = \sum_{b,k} \|\tilde{\mathbf{v}}_{b,k}\|_2^2 = \sum_{b,k} 1/\gamma_{b,k}^2 \|\tilde{\mathbf{w}}_{b,k}\|_2^2$. In this "adaptive ridge" formulation the elements of $\mathbf{\Gamma}$, which in our methods we learn, act as weights for the ℓ_2 regularization of \mathbf{W} . Equivalently, we can see this as the Bayesian

⁴If $r = K$ we disentangle the model learning into K independent learning tasks; if $r = 1$ we fall back onto F-VAR.

maximum-a-posteriori with Gaussian priors where the elements of $\mathbf{\Gamma}$ are the learned priors for the variance of the model parameters or (perhaps more interestingly) the random errors.

3 Related work

In traditional statistical approach the structure of the VAR model is controlled by restricting certain parameter values to zero based either on the subject matter theory or after using a series of tests on restricted and unrestricted models, which is gravely impractical for VARs of bigger sizes, e.g. [1].

Bayesian methods integrating domain knowledge into the VAR learning have recently seen some resurgence, e.g. [8, 9, 10], though without the aim and ability to discover the G-causal relationships since the Gaussian and inverted Wishart priors explored in these papers do not yield sparse models.

Outside the VAR world, the literature on variable selection and on promoting specific structures in the models is vast. Various classical forms of structured sparsity-inducing norms (reviewed in [11]) have been picked up for the VARs. [12] and [13] used the group lasso penalty of [14], though by applying it to each learning task independently they ignored the possible existence of common structures in the multiple time series system which we exploit by the joint model learning. [15] suggested to use the multivariate group lasso of [2] applied on the rows of the parameters matrix. However, the row sparsity they have achieved does not ensure sparsity in the G-causal graphs. In [16], based on similar motivation as ours, the authors recover a sparse dependency structure amongst the time series after removing global low-rank latent effect. However, their method works with only single lag dependencies and has no ability to cluster models as it assumes global effect of the common latent factors across all the models.

In the standard multi-task setting, a similar decomposition as in our equation (3) was used in [17] and [18]. In the first in combination with the row-wise multivariate group lasso penalty to learn sparse models over common features. In the second, to allow for common and task-specific model effects in the sparse model learning over groups of features. However, neither of these uses the notion of G-causality and the methods have no capability for model clustering based on locality of the common effects.

The problem of learning the model clustering (as opposed to learning a priori clustered models) has been addressed from rather different perspectives. In [19], the authors learn task-clustering as mixtures of cluster-specific Gaussian priors in the hidden-to-output weights in a single-layer neural network. In [20], they use the Dirichlet priors to cluster a set of classification tasks with the same prior parametrizations together. In [3], they cluster the tasks by a K-means-like procedure based on the Euclidean distance between the task parameters but without any notion of parameters structure (groups) and not promoting sparsity.

More recently, [21] used integer programming and [4] low-rank decomposition of the parameters matrix to introduce task clustering into the common features learning of [17]. While the latter is similar to our method in terms of the interpretation of the low-rank decomposition as a soft-clustering of the models, their method has no capability for promoting sparsity or structure in the parameters matrix \mathbf{W} .

4 Experiments

In our experiments, we compare the efficiency of our methods against several baseline methods in terms of the a) predictive performance, and b) the ability to discover sparse focalised G-causality graphs.

We conduct our experiments on three real datasets: based on the US macro-economic data of [22] (typically used as a benchmarking dataset by the time-series community) we construct E-20 dataset with $K = 20$ major economic indicators and E-40 with $K = 40$ adding further 20 aggregated series (both quarterly, 1959:Q1-2008:Q4); F-51 dataset has $K = 51$ series of Google Flu Trends influenza activity estimates in the US (<http://www.google.org/flutrends>) (weekly, 2003:W40-2015:W3). All datasets are seasonally adjusted and transformed to stationarity (by differencing or log-differencing) by applying preprocessing steps derived from [22] (full list of indicators and transformations is in the appendix).

For evaluating the performance we learn 100 models over sliding windows of 10 years of data (3 years for the influenza data) for each of the compared methods. We standardize the data in each of the windows by removing the mean and dividing by the standard deviation. We fix the number of lags at $p = 5$ for all our experiments and all the methods and tune the other regularization hyper-parameters of all the methods (our methods as well as the benchmarks) and the number of ranks in SF-VAR by 5-folds inner cross-validation (searching through grids typically over $10^{[-3:0.5:5]}$)⁵. For the non-convex F-VAR and SF-VAR methods we find a local solution from a single run (see sections 2.1 and 2.2 for the initialisation).

We compare our methods (F-VAR and SF-VAR) with predicting the mean (Mean), the previous value (RW) and the autoregressive fit (AR) as simple baselines. We use VAR with the standard ridge [6] penalty (RdgVAR), single feature lasso [23] (LssVAR), and group lasso [14] (GlssVAR) with groups defined as the p -long feature sub-vectors as benchmark VAR methods⁶. We use two multi-task benchmark methods: the multivariate group lasso of [2] applied to rows of \mathbf{W} (MglssVAR) and the clustered multi-task regression of [3] (CmtVAR)⁷.

It is important to note that none of the above baselines has all the capabilities we ask from our methods. The RdgVAR and LssVAR follow rather simple assumptions on the size or sparsity of the model parameters but have no further structural assumptions and do not allow the models to share information via joint learning. Likewise, no information is being shared amongst the models in the structure aware GlssVAR. The MglssVAR ties the model learning together but without supporting the block-structures and without any cluster learning ability. The CmtVAR learns the parameters together with the model clustering but does not encourage sparsity or any of the structural assumptions of our methods.

4.1 Experimental results

We evaluate the predictive performance of the tested methods using the mean squared error (MSE) of one-step-ahead forecasts averaged over 100 sliding hold-out points. We measure the structural performance of the methods by calculating the average number of active edges (as % of fully connected graph) and the average number of focal series in the G-causal graphs they discover (in addition to the dependency of each series on its own past included by default). The results are summarised in table 1.

Table 1: Summary comparison of experimental results

	MSE			Edges(%)			Focal series(#)		
	E-20	E-40	F-51	E-20	E-40	F-51	E-20	E-40	F-51
Mean	1.22*	1.10*	1.04*	not relevant					
RW	1.76*	1.47*	1.53*						
AR	0.95	0.84	1.03*						
RdgVAR	0.98*	0.87	0.89	100	100	100	20	40	51
LssVAR	1.00*	0.88	0.99*	36.6	34.7	46.1	20	40	51
GlssVAR	0.98*	0.85	0.97*	28.2	27.3	46.4	20	40	51
MglssVAR	1.02*	0.87	0.89	72.5	70.8	89.7	14.5	28.3	45.8
CmtVAR	1.00*	0.87	0.92	100	100	100	20	40	51
F-VAR	0.93	0.86	0.90	6.0	2.9	2.7	1.2	1.1	1.4
SF-VAR	0.92	0.86	0.90	5.4	2.7	2.2	1.1	1.1	1.2

(*) method significantly worse than SF-VAR in a one-sided pair-wise t-test at $\alpha=0.05$.

In each experiment the method with the lowest average MSE is in bold.

Our methods forecast significantly better than the simple Mean and RW baselines on all three datasets we experiment with. In comparison with the other benchmark methods, the predictive

⁵Details on the search grids are in the annex.

⁶All of these can be decomposed into K independent problems learned in a single-task manner.

⁷We have adapted the implementation of the convex relaxation method published on the authors' web page to fit our experimental set-up.

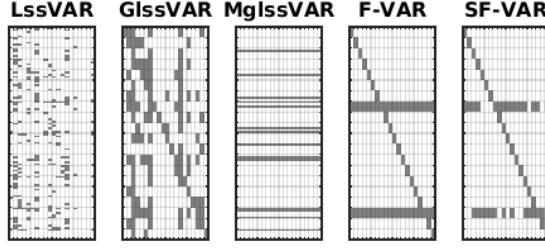


Figure 3: Example of the learned parameter matrices \mathbf{W} in the E-20 experiment (for the 50th sliding window). Shaded cells are non-zero elements. Showing only sparse methods.

Table 2: Stability of sparse selection

	Avg similarity		
	E-20	E-40	F-51
LssVAR	0.16	0.14	0.34
GlssVAR	0.28	0.24	0.40
MglssVAR	0.28	0.30	0.56
F-VAR	0.69	0.63	0.82
SF-VAR	0.65	0.63	0.79

The similarity takes values in $[-1, 1]$ reaching 1 when selected feature sets are identical.

performance of our methods is always better or comparable⁸ while the discovered G-causal graphs are notably sparser with much lower percentages of active edges and numbers of focal series.

Figure 3 depicts the learned \mathbf{W} matrices of benchmark sparse VAR learning methods and our methods for the E-20 experiment (for the 50th sliding window). It illustrates how the constraints imposed on our F-VAR and SF-VAR method yield patterns (shaded cells) consistent with our structural assumptions (see figure 1(a) and the discussion in section 2.1 and 2.2) while the G-causal graphs corresponding to the learned parameters of the other methods are much denser. It also shows the local effect of the focal series limited to only some models (clusters) in the SF-VAR method as compared to single global effect in the F-VAR. Unlike in F-VAR (where the 8th and the 18th are the focal series used in all the models), in SF-VAR both the focal series are used in the models for tasks $\{3, 4, 10, 12, 15, 17\}$ (though with task-specific weights), while models $\{1, 2, 9, 11, 13, 14, 18, 20\}$ use only the 8th series and the remaining tasks only the 18th series as inputs.

Finally, we explore in table 2 the feature selection stability of the sparse methods using the measure of [24] based on the average pair-wise intersection of the selected feature sets corrected for chance and cardinality (see the appendix for details). Using this measure, the stability of our methods across the 100 sliding windows in our experimental datasets is about double that of the baseline sparse VAR methods.

5 Conclusions

Vector autoregressive models have an inherent structure (which corresponds to the associations between the time-series in terms of which series is useful for forecasting which other series) that has been largely ignored by existing VAR learning methods.

In this paper we address these structures within VARs head-on and develop methods that explicitly account for them in the learning process. The models we learn can be described by focalised G-causality graphs, i.e. we learn sparse VARs in which the models use only small numbers of focal time-series.

We have developed two VAR methods that differ in the assumptions they make on the sharing of the focal series amongst the models of the individual series predictive tasks. The first method, Focalised-VAR, assumes that there is a single set of a few focal series that are present in all the models. The second method, SoftFocalised-VAR, relaxes this assumption and allows for different sets of the focal series to be combined and generate the individual time-series models.

In a set of experiments our methods systematically outperform (or are on par with) the state-of-the-art sparse VAR methods, while, at the same time, they uncover focalised G-causality graphs with levels of sparsity that are far beyond what any of the competing methods can do.

Both our methods can also be seen as methods for learning structured sparsity in a multi-task setting. Consequently, their applicability can be extended beyond the specific VAR setting to other problems with similar requirements.

⁸When other methods perform better the difference is never statistically significant in favour of the other methods.

References

- [1] Helmut Lütkepohl. *New introduction to multiple time series analysis*. Springer-Verlag Berlin Heidelberg, 2005.
- [2] Guillaume Obozinski, Martin J. Wainwright, and Michael I. Jordan. Support union recovery in high-dimensional multivariate regression. *The Annals of Statistics*, 39(1):1–47, February 2011.
- [3] Laurent Jacob, Francis Bach, and JP Vert. Clustered multi-task learning: A convex formulation. In *Advances in Neural Information Processing Systems (NIPS)*, 2009.
- [4] Abhishek Kumar and Hal Daume III. Learning task grouping and overlap in multi-task learning. In *International Conference on Machine Learning (ICML)*, 2012.
- [5] CWJ Granger. Investigating causal relations by econometric models and cross-spectral methods. *Econometrica: Journal of the Econometric Society*, 37(3):424–438, 1969.
- [6] Arthur E. Hoerl and Robert W. Kennard. Ridge regression: biased estimation for nonorthogonal problems. *Technometrics*, 12(1):55–67, 1970.
- [7] Amir Beck and Marc Teboulle. Gradient-based algorithms with applications to signal recovery. *Convex Optimization in Signal Processing and Communications*, 2009.
- [8] Marta Banbura, Domenico Giannone, and Lucrezia Reichlin. Large Bayesian vector auto regressions. *Journal of Applied Econometrics*, 25(November 2009):71–92, 2010.
- [9] Andrea Carriero, Todd E. Clark, and Massimiliano Marcellino. Bayesian VARs: specification choices and forecast accuracy. *Journal of Applied Econometrics*, 2013.
- [10] Gary Koop. Forecasting with medium and large Bayesian VARs. *Journal of Applied Econometrics*, 203(28):177–203, 2013.
- [11] Francis Bach, Rodolphe Jenatton, Julien Mairal, and Guillaume Obozinski. Structured sparsity through convex optimization. *Statistical Science*, 27(4):450–468, November 2012.
- [12] Aurélie C Lozano, Naoki Abe, Yan Liu, and Saharon Rosset. Grouped graphical Granger modeling for gene expression regulatory networks discovery. *Bioinformatics (Oxford, England)*, 25(12), June 2009.
- [13] Jitkomut Songsiri. Sparse autoregressive model estimation for learning Granger causality in time series. In *Proceedings of the 38th IEEE International Conference on Acoustics, Speech, and Signal Processing (ICASSP)*, 2013.
- [14] Ming Yuan and Yi Lin. Model selection and estimation in regression with grouped variables. *Journal of the Royal Statistical Society: Series B (Statistical Methodology)*, 68(1):49–67, 2006.
- [15] Song Song and Peter J. Bickel. Large vector auto regressions. *arXiv preprint arXiv:1106.3915*, 2011.
- [16] Ali Jalali and Sujay Sanghavi. Learning the dependence graph of time series with latent factors. In *International Conference on Machine Learning (ICML)*, 2012.
- [17] Andreas Argyriou, Theodoros Evgeniou, and Massimiliano Pontil. Convex multi-task feature learning. *Machine Learning*, 73(3):243–272, January 2008.
- [18] Grzegorz Swirszcz and Aurelie C. Lozano. Multi-level lasso for sparse multi-task regression. In *International Conference on Machine Learning (ICML)*, pages 361–368, 2012.
- [19] Bart Bakker and Tom Heskes. Task clustering and gating for bayesian multitask learning. *Journal of Machine Learning Research*, 4:83–99, 2003.
- [20] Ya Xue, Xuejun Liao, Lawrence Carin, and Balaji Krishnapuram. Multi-task learning for classification with Dirichlet process priors. *Journal of Machine Learning Research*, 8:35–63, 2007.
- [21] Zhuoliang Kang, Kristen Grauman, and Fei Sha. Learning with whom to share in multi-task feature learning. In *International Conference on Machine Learning (ICML)*, 2011.
- [22] James H. Stock and Mark W. Watson. Generalized shrinkage methods for forecasting using many predictors. *Journal of Business & Economic Statistics*, 30(4):481–493, October 2012.
- [23] Robert Tibshirani. Regression shrinkage and selection via the lasso. *Journal of the Royal Statistical Society. Series B*, 58(1):267–288, 1996.
- [24] Sarah Nogueira and Gavin Brown. Measuring the stability of feature selection with applications to ensemble methods. In *Intl Workshop on Multiple Classifier Systems*, 2015.

Appendix

A Stability measure

To measure the stability of the feature selection (table 2 in section 4.1) we calculate the average of pairwise similarities in the selected feature sets across the 100 sliding windows used in our experiments. The similarity between two selected feature sets s_1 and s_2 is defined as in [24]

$$S(s_1, s_2) = \frac{r - E(r)}{\max(|r - E(r)|)}, \quad (6)$$

where $r = |s_1 \cap s_2|$ is the size of the intersection of the selected features, and $E(r) = k_1 k_2 / d$ is the expected size of the intersection if drawing the same number of features $k_1 = |s_1|$ and $k_2 = |s_2|$ as in the two compared sets out of the total d features at random. This measure allows us to compare the stability of the feature selection across the tested methods as it corrects for chance in selecting feature sets of unequal sizes.

B Regularization hyper-parameters

In the experiments in section 4, we tune the hyper-parameters of the various methods by searching through grids in 5-folds inner cross-validation. We use the same grid $\{0.001, 0.003, 0.01, 0.03, 0.1, 0.3, 1, 3, 10, 30, 100, 300, 1000, 3000, 10000, 30000, 100000\}$ for the single tuning parameter in RdgVAR, LssVAR, MglssVAR and F-VAR in all our experiments. We use the same grid also for SF-VAR where for the other parameter (rank) we search through $\{2, 3, 5, 8, 15\}$. For the 2 tuning parameters in the GlssVAR (for groups of own and other series history) we search through $\{0.001, 0.01, 0.1, 1, 10, 100, 1000, 10000\}$ for both. Finally, in the the CmtVAR the grid for the rank is the same as for SF-VAR and the other 2 tuning parameters use $\{1e-08, 1e-06, 0.001, 0.1, 0.5\}$.

C Experimental data and transformations

Table 3 lists the macro-economic indicators of [22] used in our experiments in section 4. The assignments to E-20 and E-40 datasets follow the groupings used in [10]. Before using in the experiments, we have applied the same pre-processing steps as in [22]. We have transformed the monthly data to quarterly by taking the quarterly averages (column Q in table 3); applied the stationarizing transformations described in table 4 (column T in table 3); cleaned the data from outliers by replacing observations with absolute deviations from median larger than 6 times the interquartile range by the median of the 5 preceding values. The F-51 data are stationarised by taking the 52nd and 1st differences and cleaned from outliers by the same procedure as for E-20 and E-40.

Table 3: Macro-economic data and transformations

Code	Exp	Q	T	Description
GDP251	E-20	Q	5	real gross domestic product, quantity index (2000=100) , saar
CPIAUCSL	E-20	M	6	cpi all items (sa) fred
FYFF	E-20	M	2	interest rate: federal funds (effective) (% per annum,nsa)
PSCCOMR	E-20	M	5	real spot market price index:bls & crb: all commodities(1967=100)
FMRNBA	E-20	M	3	depository inst reserves:nonborrowed,adj res req chgs(mil\$,sa)
FMRRA	E-20	M	6	depository inst reserves:total,adj for reserve req chgs(mil\$,sa)
FM2	E-20	M	6	money stock:m2(m1+o'nite rps,euro\$,g/p& b/d mmmfs& sav& sm time dep
GDP252	E-20	Q	5	real personal consumption expenditures, quantity index (2000=100) , saar
IPS10	E-20	M	5	industrial production index - total index
UTL11	E-20	M	1	capacity utilization - manufacturing (sic)
LHUR	E-20	M	2	unemployment rate: all workers, 16 years & over (% ,sa)
HSFR	E-20	M	4	housing starts:nonfarm(1947-58),total farm& nonfarm(1959-)
PWFSA	E-20	M	6	producer price index: finished goods (82=100,sa)
GDP273	E-20	Q	6	personal consumption expenditures, price index (2000=100) , saar
CES275R	E-20	M	5	real avg hrly earnings, prod wrkrs, nonfarm - goods-producing

Continued on next page

Table 3 – Continued from previous page

Code	Exp	Q	T	Description
FM1	E-20	M	6	money stock: m1(curr,trav.cks,dem dep,other ck'able dep)(bil\$,sa)
FSPIN	E-20	M	5	s& p's common stock price index: industrials (1941-43=10)
FYGT10	E-20	M	2	interest rate: u.s.treasury const maturities,10-yr.(% per ann,nsa)
EXRUS	E-20	M	5	united states,effective exchange rate(merm)(index no.)
CES002	E-20	M	5	employees, nonfarm - total private
GDP251	E-40	Q	5	real gross domestic product, quantity index (2000=100) , saar
CPIAUCSL	E-40	M	6	cpi all items (sa) fred
FYFF	E-40	M	2	interest rate: federal funds (effective) (% per annum,nsa)
PSCCOMR	E-40	M	5	real spot market price index:bls & crb: all commodities(1967=100)
FMRNBA	E-40	M	3	depository inst reserves:nonborrowed,adj res req chgs(mil\$,sa)
FMRRA	E-40	M	6	depository inst reserves:total,adj for reserve req chgs(mil\$,sa)
FM2	E-40	M	6	money stock:m2(m1+o'nite rps,euro\$,g/p& b/d mmmfs& sav& sm time dep
GDP252	E-40	Q	5	real personal consumption expenditures, quantity index (2000=100) , saar
IPS10	E-40	M	5	industrial production index - total index
UTL11	E-40	M	1	capacity utilization - manufacturing (sic)
LHUR	E-40	M	2	unemployment rate: all workers, 16 years & over (% ,sa)
HSFR	E-40	M	4	housing starts:nonfarm(1947-58),total farm& nonfarm(1959-)
PWFSA	E-40	M	6	producer price index: finished goods (82=100,sa)
GDP273	E-40	Q	6	personal consumption expenditures, price index (2000=100) , saar
CES275R	E-40	M	5	real avg hrly earnings, prod wrks, nonfarm - goods-producing
FM1	E-40	M	6	money stock: m1(curr,trav.cks,dem dep,other ck'able dep)(bil\$,sa)
FSPIN	E-40	M	5	s& p's common stock price index: industrials (1941-43=10)
FYGT10	E-40	M	2	interest rate: u.s.treasury const maturities,10-yr.(% per ann,nsa)
EXRUS	E-40	M	5	united states,effective exchange rate(merm)(index no.)
CES002	E-40	M	5	employees, nonfarm - total private
SFYGT10	E-40	M	1	fygt10-fygm3
HHSNTN	E-40	M	2	u. of mich. index of consumer expectations(bcd-83)
PMI	E-40	M	1	purchasing managers' index (sa)
PMDEL	E-40	M	1	napm vendor deliveries index (percent)
PMCP	E-40	M	1	napm commodity prices index (percent)
GDP256	E-40	Q	5	real gross private domestic investment, quantity index (2000=100) , saar
LBOUT	E-40	Q	5	output per hour all persons: business sec(1982=100,sa)
PMNV	E-40	M	1	napm inventories index (percent)
GDP263	E-40	Q	5	real exports, quantity index (2000=100) , saar
GDP264	E-40	Q	5	real imports, quantity index (2000=100) , saar
GDP265	E-40	Q	5	real government consumption expenditures & gross investment
LBMNU	E-40	Q	5	hours of all persons: nonfarm business sec (1982=100,sa)
PMNO	E-40	M	1	napm new orders index (percent)
CCINRV	E-40	M	6	consumer credit outstanding - nonrevolving(g19)
BUSLOANS	E-40	M	6	commercial and industrial loans at all commercial banks (fred) billions
PMP	E-40	M	1	napm production index (percent)
GDP276_1	E-40	Q	6	housing price index
GDP270	E-40	Q	5	real final sales to domestic purchasers, quantity index (2000=100) , saar
GDP253	E-40	Q	5	real personal consumption expenditures - durable goods
LHEL	E-40	M	2	index of help-wanted advertising in newspapers (1967=100,sa)

Table 4: Stationarizing transformations

T	Transformation
1	$y_t = z_t$
2	$y_t = z_t - z_{t-1}$
3	$y_t = (z_t - z_{t-1}) - (z_{t-1} - z_{t-2})$
4	$y_t = \log(z_t)$
5	$y_t = \ln(z_t/z_{t-1})$
6	$y_t = \ln(z_t/z_{t-1}) - \ln(z_{t-1}/z_{t-2})$

z_t is the original data, y_t is the transformed series